Received 10 March 2020; accepted 3 April 2020. Date of publication 8 April 2020; date of current version 7 May 2020.
The review of this article was arranged by Editor T.-L. Ren.

Digital Object Identifier 10.1109/JEDS.2020.2986172

Performance Investigation of an n-Type Tin-Oxide Thin Film Transistor by Channel Plasma Processing

Z. W. SHANG[1], J. MA[1], W. D. LIU[1], Y. C. FAN[2], H. H. HSU[2], Z. W. ZHENG[1], AND C. H. CHENG[3]

1 School of Electronic Science and Engineering, Xiamen University, Xiamen 361005, China
2 Department of Materials and Mineral Resources Engineering, National Taipei University of Technology, Taipei 10608, Taiwan
3 Department of Mechatronic Engineering, National Taiwan Normal University, Taipei 10610, Taiwan

CORRESPONDING AUTHORS: H. H. HSU (e-mail: hhhsu@mail.ntut.edu.tw), Z. W. ZHENG (e-mail: zwzheng@xmu.edu.cn)

This work was supported in part by the National Natural Science Foundation of China under Grant 61704141, and in part by the Fundamental Research Funds for the Central Universities under Grant 20720190143.

ABSTRACT In this paper, we investigated the performance of an n-type tin-oxide (SnO_x) thin film transistor (TFT) by experiments and simulation. The fabricated SnO_x TFT device by oxygen plasma treatment on the channel exhibited n-type conduction with an on/off current ratio of 4.4x10^4, a high field-effect mobility of 18.5 cm^2/V.s and a threshold swing of 405 mV/decade, which could be attributed to the excess reacted oxygen incorporated to the channel to form the oxygen-rich n-type SnO_x. Furthermore, a TCAD simulation based on the n-type SnO_x TFT device was performed by fitting the experimental data to investigate the effect of the channel traps on the device performance, indicating that performance enhancements were further achieved by suppressing the density of channel traps. In addition, the n-type SnO_x TFT device exhibited high stability upon illumination with visible light. The results show that the n-type SnO_x TFT device by channel plasma processing has considerable potential for next-generation high-performance display application.

INDEX TERMS Thin film transistor (TFT), tin-oxide (SnO_x), plasma, TCAD.

I. INTRODUCTION

Oxide-based semiconductor thin film transistors (TFTs), such as ZnO, IGZO [1]–[5], have attracted much attention and been widely studied for high-performance display applications, owing to their high mobility, good transparency and low temperature process as compared with amorphous and poly-silicon TFTs [6]–[7]. However, most of them exhibited n-type conduction and the performance of p-type oxide-based TFTs still lag behind due to the lack of p-type oxide with high hole mobility. In recent years, tin-oxide (SnO_x) semiconductor materials with high intrinsic mobility have been demonstrated in p-type TFT devices and the n-type polarity was also revealed in oxygen-rich SnO_x condition [8]–[17], which makes both n-type and p-type property possible in the same material. It is an important characteristic for realizing power-efficient transparent circuits by a simple process. Therefore, it is imperative to develop bipolar oxide semiconductors like SnO_x to allow the fabrication of more compact CMOS devices. We previously have demonstrated p-type SnO_x TFT devices using the fluorine plasma treatment on the channel [18]. Base on this approach of channel plasma processing, in this work, we fabricated an n-type SnO_x TFT device with oxygen plasma treatment on the channel, which exhibited an on/off current ratio (I_{on}/I_{off}) of 4.4x10^4, a high field-effect mobility (μ_{FE}) of 18.5 cm^2/V.s and a threshold swing (*SS*) of 405 mV/decade. To further improve the device performance, we performed a TCAD simulation based on the experimental data to investigate the effect of the channel traps, which provided an efficient and economical way to understand the routes of electrical performance improvements. Furthermore, since TFTs used for full transparent active-matrix display are inevitably exposed to backlight during operation, it is of crucial significance to investigate the reliability properties under various

This work is licensed under a Creative Commons Attribution 4.0 License. For more information, see https://creativecommons.org/licenses/by/4.0/

light illumination conditions. High stability upon illumination with visible light was achieved in our n-type SnO_x TFT device, which is very beneficial for high-performance display application in the future.

II. EXPERIMENTS

The proposed bottom-gate n-type SnO_x TFT devices were fabricated on an n^+-type silicon substrate. First, a 50-nm-thick high-κ HfO_2 was deposited by an e-beam evaporation system as the gate dielectric, followed by a 400°C post deposition annealing (PDA) in the nitrogen ambient for 20 minutes to initiate dielectric activation. Subsequently, an 8-nm-thick SnO_x was dc-sputtered by the Sn target in the oxygen ambient as the active channel layer, followed by 200°C PDA in the nitrogen ambient for 30 minutes. Then, the SnO_x channel layer was treated using the oxygen plasma unit in a reactive-ion-etching (RIE) system with a pressure of 10 mTorr. Finally, 50-nm-thick low-cost Ni metals were evaporated by e-beam and patterned by shadow mask to form the source and drain contact electrodes. The n^+-type silicon was used as both the substrate and the gate electrode. The TFT devices have a channel width (W) of 520 μm and a channel length (L) of 60 μm. For comparison, the SnO_x TFT devices without the oxygen plasma treatment were also fabricated. In addition, a high capacitance density of ~0.3 $\mu F/cm^2$ was obtained for the $Ni/HfO_2/n^+$-Si MIS gate capacitors, which were fabricated alongside the transistors. The electrical characteristics of the TFT devices were measured by HP 4156C semiconductor parameter analyzer at room temperature. The red-green-blue (RGB) light illumination was provided by a bandpass halogen lamp with the same illumination intensity of 6 mW/cm^2. For the device simulation, it was performed by utilizing Synopsys Sentaurus device simulator. The models used in the simulation were Shockley-Read-Hall (SRH) recombination, band gap narrowing and standard drift-diffusion models.

III. RESULTS AND DISCUSSION

Figure 1 shows the typical transfer $I_D - V_G$ characteristics of the SnO_x TFT device with and without the oxygen plasma treatment on the channel, and the inset shows the schematic structure of the TFT device. It was obviously observed that the SnO_x TFT device without the oxygen plasma treatment on the channel exhibited p-type conduction. However, after applying the oxygen plasma treatment on the channel, the TFT device showed n-type conduction, which can be ascribed to the excess oxygen incorporated to the channel and converted oxygen-deficient p-type SnO_x (Sn^{2+} preferred) to oxygen-rich n-type SnO_x (Sn^{4+} preferred) [11]. For the TFT device characteristics, I_{on}/I_{off} can be obtained from the $I_D - V_G$ curve and μ_{FE} can be extracted from a gradual channel approximation in the linear region according to the equation [19]:

$$\mu_{FE}=\frac{\partial I_D}{\partial V_G}\cdot\frac{L}{W}\cdot\frac{1}{V_D\cdot C_G} \tag{1}$$

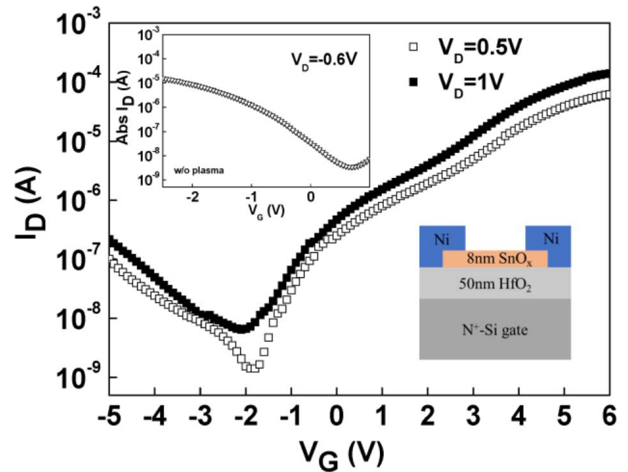

FIGURE 1. Typical transfer $I_D - V_G$ characteristics of the SnO_x TFT device with and without the oxygen plasma treatment on the channel, and the schematic structure of the TFT device in the inset.

where C_G is the gate insulator capacitance per unit. For the n-type SnO_x TFT device, it showed the performances with an I_{on}/I_{off} of 4.4x10^4, an SS of 405 mV/decade, and a high μ_{FE} of 18.5 $cm^2/V.s$ at the drain voltage of 0.5 V. In addition, it is well known that the characteristics of the TFT devices are strongly influenced by the interface trap states at the interface between the gate insulator and the active channel layer, because the field-induced carriers are confined in a very thin region close to the interface. The interface defects can produce trapping or scattering effects, resulting in SS degradation. For the TFT device, the density of interface traps (N_{it}) at the gate insulator/active channel interface can be extracted from the equation [20]:

$$N_{it}=\left[\mathrm{SS}\cdot\log(e)\cdot\frac{q}{kT}-1\right]\cdot\frac{C_G}{q} \tag{2}$$

where k, q and T are the Boltzmann constant, the charge quantity of an electron and the absolute temperature, respectively. For the fabricated n-type SnO_x TFT device, an N_{it} value of 1.1x10^{13} cm^{-2} was obtained, resulting in a moderate SS of 405 mV/dec. Besides, it was found that a hump occurred in the transfer curve for the n-type SnO_x TFT device, which could be due to the deep-level acceptor-like states induced by the oxygen plasma process [21].

To further improve the performance of the n-type SnO_x TFT device, we investigated the effect of the density of channel traps with different levels on the electrical characteristics of the n-type SnO_x TFT devices by TCAD simulation tools. The parameters of TFT models were decided by the experimental data. Figure 2 shows the measured and simulated transfer characteristic of the n-type SnO_x TFT devices with different densities of the channel traps. It can be observed the simulated $I_D - V_G$ curve of the device with the medium density of channel traps was similar with the experimental data. Device performances were evaluated by adjusting the channel trap density in the device simulation. It was notable that the off-state current and the

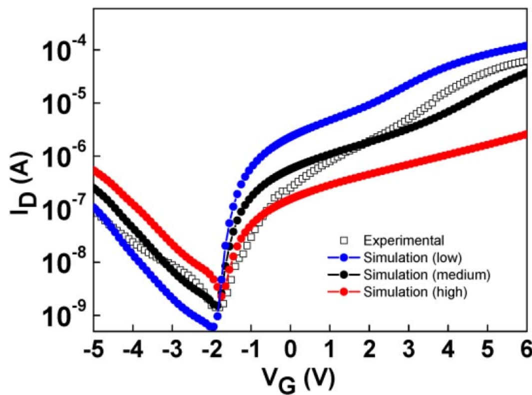

FIGURE 2. Measured and simulated transfer characteristic of the n-type SnO_x TFT devices with different densities of channel traps.

SS were obviously decreased as the density of the channel traps decreasing, thus improving the I_{on}/I_{off}. In addition, the hump was also affected by the density of the channel traps, which were mainly defined as the acceptor-like states in the simulation. As the channel trap density increased, the above-threshold region shifted more in the positive direction, which agreed well with the previous report [21]. Figure 3(a), (b), (c) and (d) show the extracted I_{on}/I_{off}, *SS* μ_{FE} and N_{it} values of the simulated n-type SnO_x TFT devices as a function of the channel trap density. These improvements in the TFT device with the low density of channel traps can be attributed to the low defect-induced current leakage and interface roughness, which agreed with the previous experimental report [18]. Therefore, it is believed that our SnO_x TFT device performance can be further optimized by improving the channel and channel/dielectric interface quality with optimal approaches of fabrication process.

To investigate the electrical stability of the n-type SnO_x TFT device under visible light illumination, we performed the electrical measurements in the dark and under the light illumination at various RGB wavelengths. Figure 4 shows the typical transfer $I_D - V_G$ characteristics of the n-type SnO_x TFT device in the dark and under light illumination at RBG wavelengths (λ), respectively, including the red-light (λ ∼ 780–620 nm), the green-light (λ ∼ 580–490 nm) and the blue-light (λ ∼ 470–420 nm). It was found that the transfer characteristics of the n-type SnO_x TFT device exposed to the red-light and green-light was almost unchanged as compared to the dark condition. With further decreasing the wavelength to the blue-light, only a slight degradation in device performances including a higher off-state current and lager *SS* was observed.

Figure 5 show the extracted read current ratio (I_{light}/I_{dark}) at the read voltage of $V_G = -1.8$ V for the n-type SnO_x TFT device. The device exhibited an I_{light}/I_{dark} of ∼2 under the illumination of red-light and green-light and a slightly larger I_{light}/I_{dark} of ∼8 under the illumination of blue-light, which was absolutely lower than that of our previous p-type SnO_x TFT device for the sensor application of the blue-light

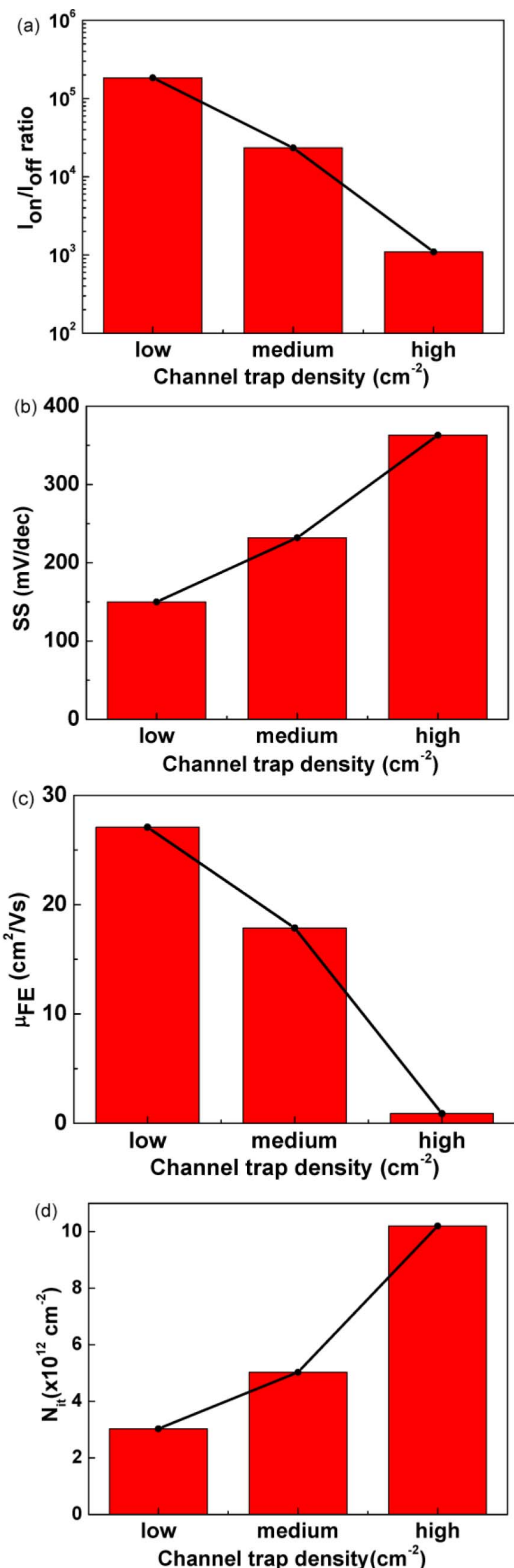

FIGURE 3. Extracted (a) I_{on}/I_{off}, (b) *SS*, (c) μ_{FE} and (d) N_{it} values of the simulated n-type SnO_x TFT devices as a function of the channel trap density.

detection [22]. It indicates that the n-type SnO_x TFT device has high stability upon the visible light. The high stability upon the visible light could be ascribed to the large

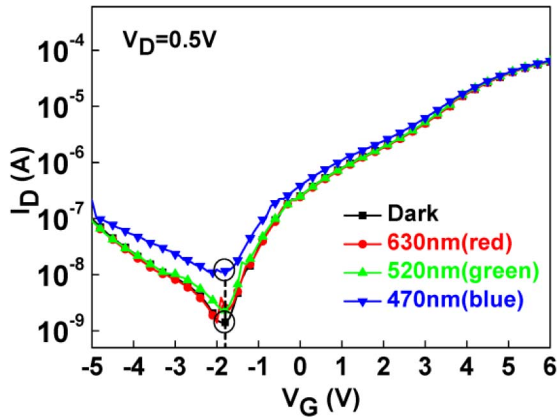

FIGURE 4. Typical transfer $I_D - V_G$ characteristics of the n-type SnO_x TFT device in the dark and under light illumination at RBG wavelengths.

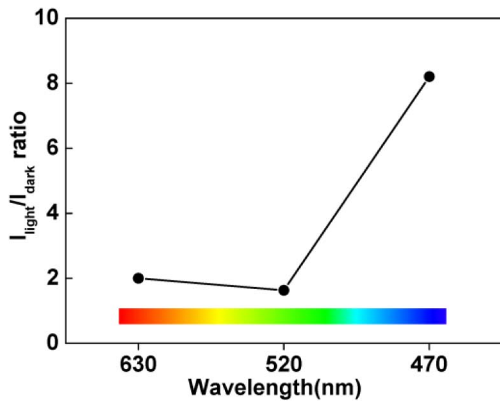

FIGURE 5. Extracted I_{light}/I_{dark} at the read voltage of $V_G = -1.8$ V for the n-type SnO_x TFT device.

bandgap of the n-type SnO_x ($\sim$3.6 eV) [23]–[25]. For the blue-light illumination, the photons has the energy of $\sim$2.6-3 eV, while for the illumination of the green-light or red-light with larger wavelength, the energy of the photons is even lower. The low photons energy is not large enough to excite the electrons directly from the valance band into the conduction band, resulting in the high stability of the device upon the visible illumination. Furthermore, we also measured the drain-source current versus drain-source voltage ($I_{DS} - V_{DS}$) curves of the n-type SnO_x TFT device in the dark and under the light illumination at RGB wavelengths, as shown in Fig. 6. It was observed that the leakage current of the n-type SnO TFT device remained almost the same under the red-light and green-light illumination as compared to that in the dark condition, and only increased slightly under the blue-light illumination, indicating no obvious carrier concentration and conduction enhancement. These results are in good agreement with the trend of I_{light}/I_{dark} as discussed above.

IV. CONCLUSION

We reported an n-type SnO_x TFT device by oxygen plasma processing on the channel and achieved high performances with an I_{on}/I_{off} of 4.4x10^4, a SS of 405 mV/decade

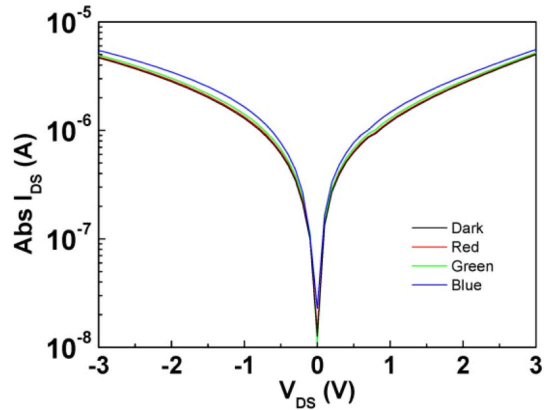

FIGURE 6. $I_{DS} - V_{DS}$ curves of the n-type SnO_x TFT device in the dark and under the light illumination at RGB wavelengths.

and a high μ_{FE} of 18.5 cm^2/V.s. More importantly, the n-type SnO_x TFT device exhibited high stability upon the visible illumination, which could be attributed to the large bandgap of the n-type SnO_x. In addition, TCAD simulation was performed to investigate the effect of the channel traps. These results show high potential and provide a solution for high-performance oxide TFTs in future high-resolution display applications.

REFERENCES

[1] K. Nomura, H. Ohta, K. Ueda, T. Kamiya, M. Hirano, and H. Hosono, “Thin-film transistor fabricated in single-crystalline transparent oxide semiconductor,” *Science*, vol. 300, no. 5623, pp. 1269–1272, May 2003.
[2] P. Barquinha *et al.*, “Gallium–indium–zinc-oxide-based thin-film transistors: Influence of the source/drain material,” *IEEE Trans. Electron Devices*, vol. 55, no. 4, pp. 954–960, Apr. 2008.
[3] H.-H. Hsu, C.-H. Cheng, P. Chiou, Y.-C. Chiu, C.-Y. Chang, and Z.-W. Zheng, “Amorphous bilayer TiO_2-InGaZnO thin film transistors with low drive voltage,” *Solid-State Electron.*, vol. 99, pp. 51–54, Sep. 2014.
[4] B. Ryu, H.-K. Noh, E.-A. Choi, and K. J. Chang, “O-vacancy as the origin of negative bias illumination stress instability in amorphous In–Ga–Zn–O thin film transistors,” *Appl. Phys. Lett.*, vol. 97, no. 2, Jul. 2010, Art. no. 022108.
[5] M.-J. Yu *et al.*, “Amorphous InGaZnO thin-film transistors compatible with roll-to-roll fabrication at room temperature,” *IEEE Electron Device Lett.*, vol. 33, no. 1, pp. 47–49, Jan. 2012.
[6] C.-W. Chen *et al.*, “High-performance hydrogenated amorphous-Si TFT for AMLCD and AMOLED applications,” *IEEE Electron Device Lett.*, vol. 26, no. 10, pp. 731–733, Oct. 2005.
[7] C.-P. Lin, B.-Y. Tsui, M.-J. Yang, R.-H. Huang, and C.-H. Chien, “High-performance poly-silicon TFTs using HfO_2 gate dielectric,” *IEEE Electron Device Lett.*, vol. 27, no. 5, pp. 360–363, May 2006.
[8] K. Nomura, T. Kamiya, and H. Hosono, “Ambipolar oxide thin-film transistor,” *Adv. Mater.*, vol. 23, pp. 3431–3434, Aug. 2011.
[9] I.-C. Chiu and I.-C. Cheng, “Gate-bias stress stability of p-type SnO thin-film transistors fabricated by RF-sputtering,” *IEEE Electron Device Lett.*, vol. 35, no. 1, pp. 90–92, Jan. 2014.
[10] J. A. Caraveo-Frescas and H. N. Alshareef, “Transparent p-type SnO nanowires with unprecedented hole mobility among oxide semiconductors,” *Appl. Phys. Lett.*, vol. 103, Nov. 2013, Art. no. 222103.
[11] P.-C. Chen *et al.*, “Bipolar conduction in tin-oxide semiconductor channel treated by oxygen plasma for low-power thin-film transistor application,” *J. Display Technol.*, vol. 12, no. 3, pp. 224–227, Mar. 2016.
[12] P.-C. Chen *et al.*, “Fast low-temperature plasma process for the application of flexible tin-oxide-channel thin film transistors,” *IEEE Trans. Nanotechnol.*, vol. 16, no. 5, pp. 876–879, Sep. 2017.

[13] H. Luo, L. Liang, H. Cao, M. Dai, Y. Lu, and M. Wang, "Control of ambipolar transport in SnO thin-film transistors by back-channel surface passivation for high performance complementary-like inverters," *ACS Appl. Mater. Interfaces*, vol. 7, no. 31, pp. 17023–17031, Aug. 2015.

[14] R. Barros *et al.*, "Role of structure and composition on the performances of p-type tin oxide thin-film transistors processed at low-temperatures," *Nanomaterials (Basel)*, vol. 9, p. 320, Jan. 2019.

[15] E. Fortunato *et al.*, "Transparent p-type SnO_x thin film transistors produced by reactive RF magnetron sputtering followed by low temperature annealing," *Appl. Phys. Lett.*, vol. 97, no. 5, Aug. 2010, Art. no. 052105.

[16] I.-C. Chiu, Y.-S. Li, M.-S. Tu, and I.-C. Cheng, "Complementary oxide–semiconductor-based circuits with n-channel ZnO and p-channel SnO thin-film transistors," *IEEE Electron Device Lett.*, vol. 35, no. 12, pp. 1263–1265, Dec. 2014.

[17] H. C. Chu, Y. S. Shen, C. H. Hsieh, J. H. Huang, and Y. H. Wu, "Low-voltage operation of ZrO_2-gated n-type thin-film transistors based on a channel formed by hybrid phases of SnO and SnO_2," *ACS Appl. Mater. Interfaces*, vol. 7, no. 28, pp. 15129–15137, Jul. 2015.

[18] P.-C. Chen, Y.-C. Chiu, Z.-W. Zheng, C.-H. Cheng, and Y.-H. Wu, "Influence of plasma fluorination on p-type channel tin-oxide thin film transistors," *J. Alloys Compound.*, vol. 707, pp. 162–166, Jun. 2016.

[19] Z. W. Zheng, C. H. Cheng, and Y. C. Chen, "Low operation voltage InGaZnO thin film transistors with $LaAlO_3$ gate dielectric incorporation," *ECS J. Solid State Sci. Technol.*, vol. 2, no. 9, pp. 179–181, Jul. 2013.

[20] P.-C. Chen, Y.-C. Chiu, G.-L. Liou, Z.-W. Zheng, C.-H. Cheng, and Y.-H. Wu, "Performance enhancements in p-type Al-doped tin-oxide thin film transistors by using fluorine plasma treatment," *IEEE Electron Device Lett.*, vol. 38, no. 2, pp. 210–212, Feb. 2017.

[21] H. Im, H. Song, J. Jeong, Y. Hong, and Y. Hong, "Effects of defect creation on bidirectional behavior with hump characteristics of InGaZnO TFTs under bias and thermal stress," *Jpn. J. Appl. Phys.*, vol. 54, no. 3S, Feb. 2015, Art. no. 03CB03.

[22] P.-C. Chen, Y.-C. Chiu, Z.-W. Zheng, C.-H. Cheng, and Y.-H. Wu, "P-type tin-oxide thin film transistors for blue-light detection application," *Physica Status Solidi Rapid Res. Lett.*, vol. 10, no. 12, pp. 919–923, Dec. 2016.

[23] Q.-J. Liu, Z.-T. Liu, and L.-P. Feng, "First-principles calculations of structural, electronic and optical properties of tetragonal SnO_2 and SnO," *Comput. Mater. Sci.*, vol. 47, no. 4, pp. 1016–1022, Feb. 2010.

[24] V. T. Agekyan, "Spectroscopic properties of semiconductor crystals with direct forbidden energy gap," *Physica Status Solidi A*, vol. 43, no. 1, pp. 11–42, Sep. 1997.

[25] L. A. Errico, "Ab initio FP-LAPW study of the semiconductors SnO and SnO_2," *Physica B, Condensed Matter*, vol. 389, no. 1, pp. 140–144, Feb. 2007.